Hindawi Publishing Corporation
Mathematical Problems in Engineering
Volume 2013, Article ID 790586, 15 pages
http://dx.doi.org/10.1155/2013/790586

Research Article

Plastic and Elastic Responses of a Jacket Platform Subjected to Ship Impacts

Liang Li,[1] Zhiqiang Hu,[1,2] and Zhe Jiang[3]

[1] *State Key Lab of Ocean Engineering, Shanghai Jiao Tong University, Shanghai 200240, China*
[2] *State Key Lab of Structure Analysis for Industrial Equipment, Dalian 20240, China*
[3] *Deepwater Engineering Key Laboratory, Technology Research Department CNOOC Research Institute, Beijing 20240, China*

Correspondence should be addressed to Zhiqiang Hu; zhqhu@sjtu.edu.cn

Received 29 June 2013; Accepted 9 August 2013

Academic Editor: Song Cen

This paper deals with ship-jacket platform collisions. An examination on NORSOK N-004 rule is carried out. Furthermore, elastic and plastic response of jacket platform is studied. This paper also conducts a sensitivity analysis, focusing on collision points. Simulation models of a ductile and a rigid supply vessel were developed, as well as models of two typical jacket platforms. Data such as collision force, kinetic energy, and deformation energy have been obtained. Several conclusions have been drawn: NORSOK rule underestimates the resistance for certain indention, due to inaccurate description of column deformation mode. Elastic response is extremely important in dynamic analysis of ship-platform impacts, by contributing to reducing impact loads and local energy dissipation. Struck members are therefore subjected to impacts to a low extent, which can be regarded as result of a buffering effect. Before a buffering effect works, a time delay exists. This is caused because the topside has to take up adequate kinetic energy. Striking position has an effect on dynamic behavior of platform. High local strength is in favor of buffering an effect. Elastic response is more significant in a flexible platform than in a sticky one.

1. Introduction

Offshore jacket platforms are widely used in the oil and gas exploration industry worldwide. Located usually many kilometers from land, jacket platforms are subjected to complex environmental loading from wind, wave action, and currents. They are also vulnerable to collision impact from supply vessels operating around them; this is one of the greatest threats to the platform's safety. Such an impact is likely to cause serious structural damage, reducing the load bearing capacity of the platform and potentially affecting the safety and integrity of the whole structure. For this reason, establishing a method of analyzing and assessing the damage to the platform is of major importance, as reflected in the large body of the literature on the subject, and in various design standards.

A detailed analysis by Amdahl [1] of the structural response of tubular structural member showed that the response of a tube to a lateral impact load is divided into two stages. The initial stage is governed by bending effects caused by local denting. In the second stage, the tube behaves in the manner of a beam and undergoes deflection, which may increase its load-bearing capacity due to the development of membrane tensile forces. When this energy is dissipated, the overall response of the platform may be neglected. Zeinoddini et al. [2] studied the behavior of steel tubes with different types of end conditions subjected to quasistatic lateral loads at their midspan. Axial preload was found to have a substantial effect on the load-bearing capacity, and the capacity for energy dissipation was influenced dramatically. They also investigated the dynamic behavior of tubes under lateral excitation [3] and found that preloading produced a much more substantial change in dynamic properties in a beam-column cylindrical member, in which global buckling is more important than in a low-aspect-ratio member.

Visser Consultancy [4] dealt with aspects related to the collision of the bow or stern of the vessel with a brace in the

splash zone and reported that node strength largely determines the load-bearing and energy-absorption capacity of the brace, concluding that brace impact is a purely local problem. Amdahl and Eberg studied the effect of dynamics on platform responses in terms of energy dissipation and load [5]. The local strength of the platform, the duration of the collision relative to the fundamental period of governing motion, and the strength of the members transmitting the forces to the deck were all found to be essential in determining the platform responses.

Bai and Terndrup Pedersen [6] studied the elastoplastic behavior of the steel structure of an offshore platform under impact loads. A force-displacement relationship was obtained for the simulation of local denting in the tube, and a three-dimensional beam-column element was developed for modeling global deflection. A large part of the impact energy was found to be transferred into plastic deformation energy in the case of a severe collision.

Pedersen and Zhang [7] developed closed-form analytical expressions for the energy dissipation and impact impulse during ship collisions. The energy dissipation depends mainly on variables such as the ship's mass and velocity, the collision location, and collision angle. Furnes and Amdahl [8] outlined a simplified theoretical calculation model for investigating deformation characteristics and energy absorption. Gjerde et al. [9] compared a range of typical methodologies used by the offshore industry to analyze the response and resistance of jack-up designs to ship impact and showed that a significant part of the collision energy was dissipated as strain energy, and the contribution from elastic strain is usually negligible. Waegter and Sterndorff [10] concentrated on the energy balance in an impact between a ship and a platform monotower. They found that little impact energy is dissipated as plastic energy in the ship-platform system in the two cases studied.

Watan [11] studied the behaviors of columns subjected to vessel collision. The assessment had been conducted for ship-side collision against unstiffened, inclined jacket leg. Hong [12] focused on the internal mechanics of ships subjected to collision and grounding accidents. Simplified methods for structural analysis were developed as well as their application to accident-resistant design. Mathematical models for ship collisions were studied by Zhang [13]. Collision energy losses, collision forces, and structural damage were determined. Wang [14] tried to identify and analyze the structural failure modes involved in ship collision and grounding.

The American Petroleum Institute (API) standards recommended two formulas for assessing collision force [15]: one of these assumes that the indentation in the steel tube is wedge-shaped and determines the extent of the indentation. The other is based on a series of model simulations. The NORSOK Standard N-004 [16] contains a recommendation for dealing with the relationship between resistance and indentation for tubes involved in a side-on collision with a ship. The dented cross-section is assumed to consist of a virtually undamaged section and a flattened section. Impact location and boundary conditions are not considered.

The above reports provide useful insights into the dynamic analysis of collisions between ships and platforms, although it should be noted that they generally tended to ignore the elastic response of the jacket platform under the assumptions that (1) the elastic response of the platform dissipates a considerable part of the impact energy, and (2) the impact loading is reduced to a low value by virtue of the buffering effect.

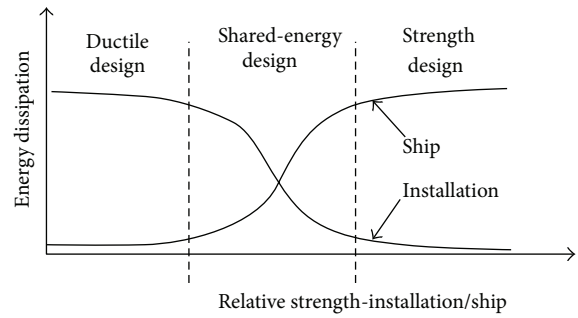

Figure 1: Schematic energy dissipation curves for strength, ductile, and shared-energy designs.

For the purpose of testing these assumptions and investigating the buffering effect, in the present study, a series of numerical simulations was conducted using LS-DYNA software. The NORSOK recommendation for the force-deformation relationship was tested by comparing numerical and simulation results from two numerical models based on typical jacket platforms, one in the South China Sea and one in Bohai Bay, China. The buffering effect was demonstrated by comparing the results from a simulated typical jacket platform with those from a single-column model. The effect of varying the impact parameters was also examined to obtain a comprehensive knowledge of the behavior of tubular members in a side-on impact. The influence of the topside on the structural response of the platform is also discussed.

2. NORSOK N-004 Standard

N-004 is a NORSOK Standard [16] dealing with the design of steel structures. Appendix A3 to N-004 dealing with ship collision contains three design principles regarding the distribution of strain energy dissipation (Figure 1):

(i) strength design,

(ii) ductility design,

(iii) shared-energy design.

Ductile Design. It implies that the installation undergoes large, plastic deformations and dissipates the major part of the collision energy.

Shared-Energy Design. It implies that both the installation and the ship contribute significantly to the energy dissipation.

Strength Design. It implies that the installation is strong enough to resist the collision force with minor deformation, so that the ship is forced to deform and dissipate the major part of the energy.

From a calculation point of view, ductile design and strength design are the most straightforward, since the

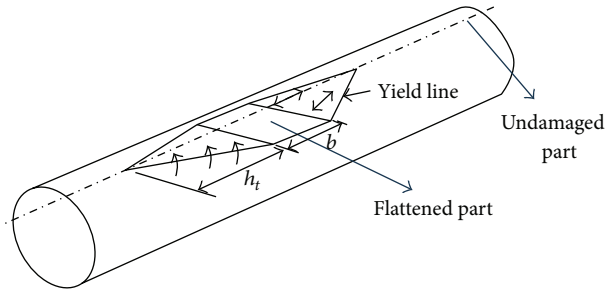

Figure 2: Yield-line model of dented tube.

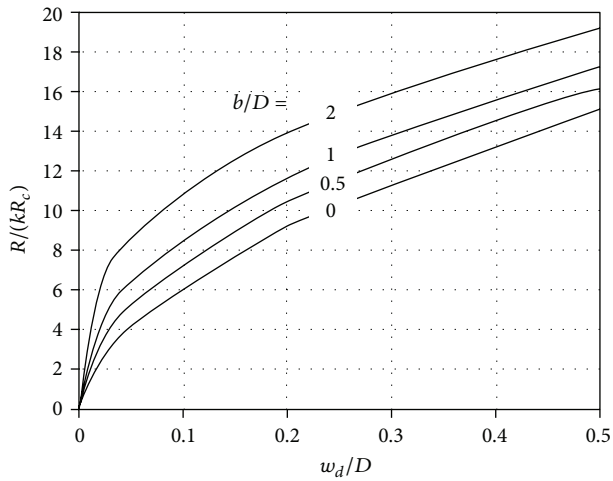

Figure 3: Resistance curve for local denting.

response of the "soft" structure can be calculated from simple considerations of the geometry of the "rigid" structure. In shared-energy design, both the magnitude and distribution of the collision forces depend on the deformation of both structures, making the analysis more complex.

A recommendation for the force-deformation relationships for denting tubular members is offered in NORSOK N-004. The deformation mode of a column in a collision, described as a dent, is assumed to consist of a flattened part and an undamaged part. The dented region is modeled by an idealized yield-line model. It is assumed that the tube is flattened at the area of direct contact with the ship and that flattening decreases in adjacent triangular regions in the direction of the fixed ends of the member (Figure 2).

Figure 3 shows the recommended resistance curve for an unstiffened column. The indentation and impact force are dimensionless.

Alternatively, the resistance may be calculated from the following:

$$\frac{R}{R_c} = kc_1\left(\frac{w_d}{D}\right)^{c_2},$$

$$R = \text{resistance force},$$

$$R_c = f_y\frac{t^2}{4}\sqrt{\frac{D}{t}},$$

$$c_1 = 22 + 1.2 \times \frac{b}{D},$$

$$c_2 = \frac{1.925}{3.5 + b/D},$$

$$\text{For } k = 1.0, \quad \frac{N_{Sd}}{N_{Rd}} \le 0.2,$$

$$\text{For } k = 1.0 - 2\left(\frac{N_{Sd}}{N_{Rd}} - 0.2\right), \quad 0.2 < \frac{N_{Sd}}{N_{Rd}} < 0.6,$$

$$\text{For } k = 0, \quad 0.6 \le \frac{N_{Sd}}{N_{Rd}}, \tag{1}$$

where N_{Sd} = design axial compressive force, N_{Rd} = design axial compressive resistance, b = width of contact area, D = diameter of column, w_d = dent depth, t = wall thickness, and f_y = yield strength.

Special attention has been paid in the present study to the following three assumptions adopted in the application of NORSOK N-004.

(1) The deformation behavior of the ship is not taken into consideration.

(2) Because of the stress concentrations, the tubes are usually strengthened near the connection points between adjacent members by increasing their wall thickness; however, in NORSOK N-004, the tube is assumed to have a single wall thickness over its full length.

(3) The elastic characteristics of the whole platform are not taken into consideration.

To evaluate these assumptions, in the present study, a series of numerical simulations were carried out.

3. Collision Scenario and Finite Element Models

In line with the stated aims of this study, numerical simulations were divided into two parts:

Part A—verifying the NORSOK Standard N-004;

Part B—investigating the buffering effect of the elastic response of the jacket platform.

3.1. Part A—Verifying NORSOK Standard N-004. The collision scenario was defined as a situation in which a supply vessel strikes a tubular leg segment of the jacket platform side-on at a constant velocity of 2 m/s.

3.1.1. Finite Element Model of Supply Vessel. In order to investigate the influence of the vessel's stiffness on the resistance-indentation relationship, both the rigid model and ductile model were used. The principal dimensions of the supply vessel are given in Table 1.

For the model, the midsection of the cargo deck was chosen as the part of the vessel that strikes the platform.

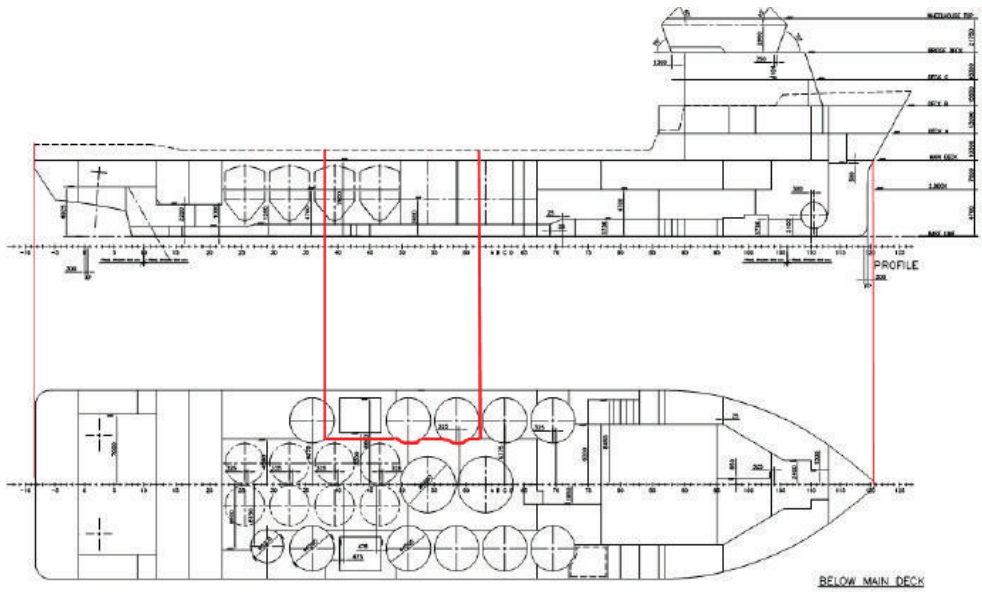

Figure 4: Supply vessel midsection model.

Table 1: Principal dimensions of reference vessel.

Length p.p.	90.90 m
Breadth, molded	18.80 m
Depth, molded	7.60 m
Draught, scantling	6.20 m

Table 2: Principal dimensions of mid-shipside model.

Length	15.60 m
Breadth	4.20 m
Height	7.60 m
Frame spacing	0.65 m
Double bottom height	1.2–1.45 mm
Thickness of outer plate	9/10.5/25 mm
Thickness of bottom plate	13.00 mm
Cross-section of side stiffeners	Hp 180 mm × 8 mm/Hp 200 mm × 9 mm

Table 2 lists the principal dimensions of the mid-section part of the vessel that was modeled. Figure 4 indicates its location on the vessel.

The nodes on the transverse edges of the ductile model, which were parallel to the impact direction, were restrained in all degrees of freedom with the exception of the translational degree of freedom parallel to the direction of the ship's motion. No boundary limitations were assigned to the nodes on the longitudinal edges, as the velocity of the ship's motion would be generated on this edge. This boundary condition was defined to ensure that the direction of motion of the vessel remained unchanged during the collision process and that no rotation of the vessel would occur. The four-node quadratic shell elements have been applied for the entire

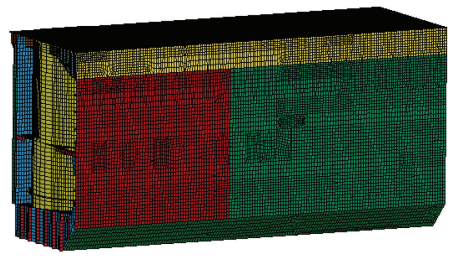

Figure 5: Ductile vessel finite element model.

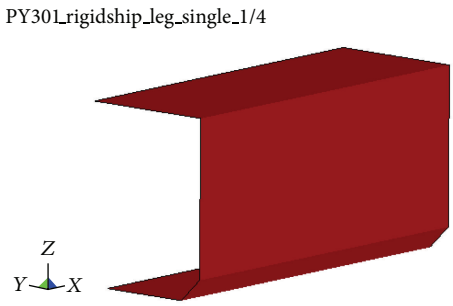

Figure 6: Rigid vessel model.

model. Element length varied between 80 mm and 150 mm for different parts, giving a total of 127, 586 elements. The ductile vessel finite element model is shown in Figure 5.

A rigid vessel model was constructed for the mid-section of the ship, as for the ductile model. However, since, by definition, the rigid model would not experience any structural deformation, only the side of the hull was included in the model for the sake of saving computation time. The principal dimensions and boundary conditions are identical to those of the ductile model. For the rigid vessel model, quad

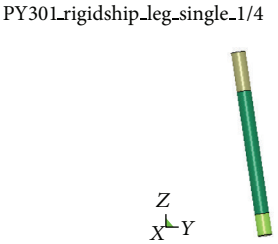

Figure 7: Leg segment I.

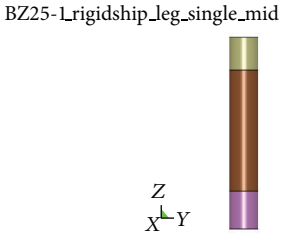

Figure 8: Leg segment II.

Table 3: Leg segment principal parameters in models.

	Model I	Model II
Length	25.00 m	17.0 m
Diameter	2.0 m	2.6 m
Wall thickness	45.0 mm	35.0 mm
Upper-end length	5.5 m	3.0 m
Upper-end wall thickness	80.0 mm	95.0 mm
Lower-end length	3.0 m	3.5 m
Lower-end wall thickness	90.0 mm	90.0 mm

Table 4: Material properties.

Mass density	7850 kg/m^3
Young's modulus	210,000 Mpa
Poisson's ratio	0.3
Yield strength	235 MPa
Strain rate parameter, C	40.4
Strain rate parameter, P	5
Static coefficient of friction	0.3
Dynamic coefficient of friction	0.3

type mesh was chosen and the global edge length is 0.5 m. The total elements number is 1,123. A coarse mesh was applied here as the hull will not undergo any deformation. Figure 6 shows the rigid vessel model.

3.1.2. Leg Segment Model. Two tubular leg segment models, I and II, were constructed. Model I was inclined from the vertical at an angle of 9.03° (Figure 7); model II was vertical (Figure 8). Both ends of each model were strengthened by increased tube wall thickness. The principal parameters of the two models are listed in Table 3.

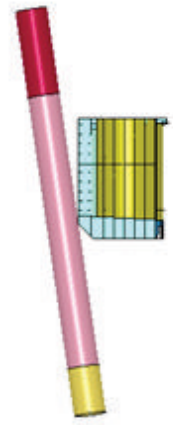

Figure 9: Midspan.

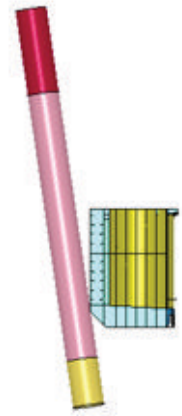

Figure 10: 1/4-span.

The lengths of the leg segments were determined on the basis of the braced length of the jacket leg subjected to ship impact. Since each leg segment was braced, it was considered reasonable to assume that its ends were fixed in all translational and rotational degrees of freedom.

For both leg segment models, the default mesh size was set to 0.01 m, and only four-node quad type mesh was allowed. Such fine mesh was applied to exactly capture the deformation behavior of impacted columns. The material chosen was Q235 structural steel. The strain rate was calculated from the Cowper-Symonds equation. The simulated material properties are listed in Table 4.

3.1.3. Collision Scenario Definition. To investigate how the vessel strength influenced the resistance-indentation relationship, numerical simulations for both ductile- and rigid-vessel crushing of leg segment I were performed. The results were compared with the recommendations of NORSOK Standard N-004.

The collision point, or first-impact point, on the ship was taken to be the point at which its lower hull first touched the

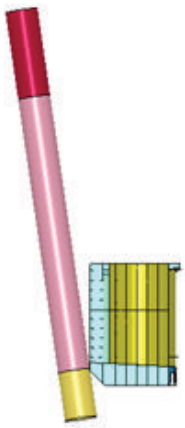

Figure 11: 1/8-span.

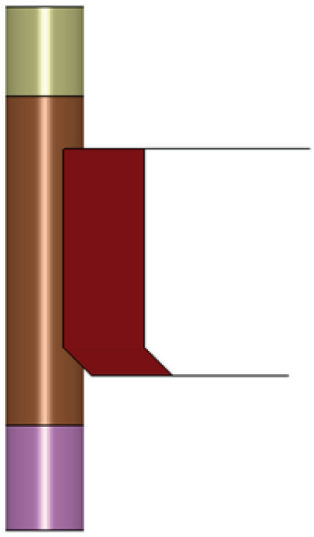

Figure 12: Mid-span location.

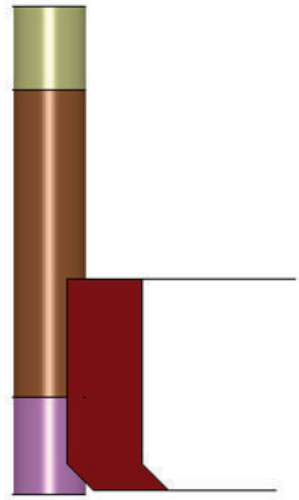

Figure 13: Lower-end location.

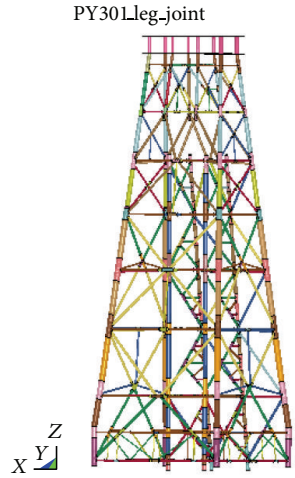

Figure 14: Platform model A.

leg segment; this was then regarded as the reference impact point.

Three collision locations were designed for leg segment I for both the rigid and ductile ship models. The same locations were defined for the simulations of jacket model A—see below.

(i) Midspan-shipside collision: reference impact point at the midpoint of leg segment I (Figure 9).

(ii) 1/4 span-shipside collision: reference impact point at 1/4 span of leg segment I (Figure 10).

(iii) 1/8 span-shipside collision: reference impact point at 1/8 span of leg segment I (Figure 11).

Simulations of vessel crushing at leg segment II were also conducted with the intention of investigating the platform's overall deformation and comparing with simulations of the behavior of the complete platform model B. Only the rigid vessel model was used in this case to minimize the calculation time.

Leg segment II was modeled to be fixed vertically, and no first-impact was assumed as was the case for segment I above. The reference collision point was chosen to be the middle of the ship's side. With respect to this reference point, two collision locations are designed.

(i) Mid-span-shipside collision: vessel impacts the mid-span of leg segment II (Figure 12).

(ii) Lower end-shipside collision: vessel impacts the lower end of leg segment II such that the bottom of the hull is leveled with the lower joint of the segment (Figure 13).

These eight collision cases are summarized in Table 5.

3.2. Part B—Elastic Response Buffering Effect. As in Section 3.1, the collision scenario was defined as the situation in which a supply vessel strikes a jacket platform at a constant velocity of 2 m/s. In an actual side-on collision, the vessel

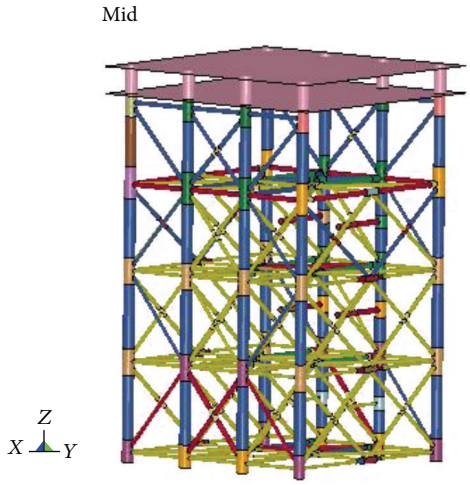

Figure 15: Platform model B.

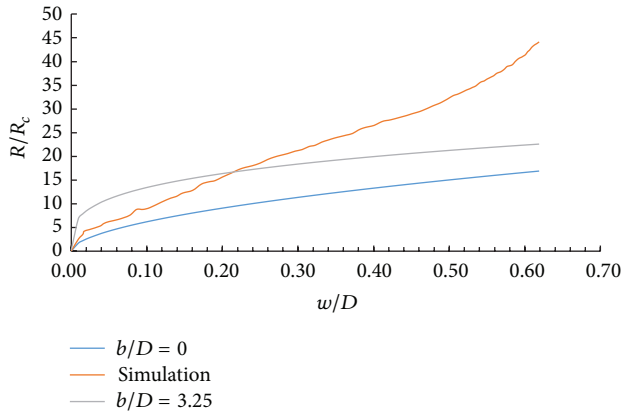

Figure 16: Comparison between Case A1 and NORSOK recommendations.

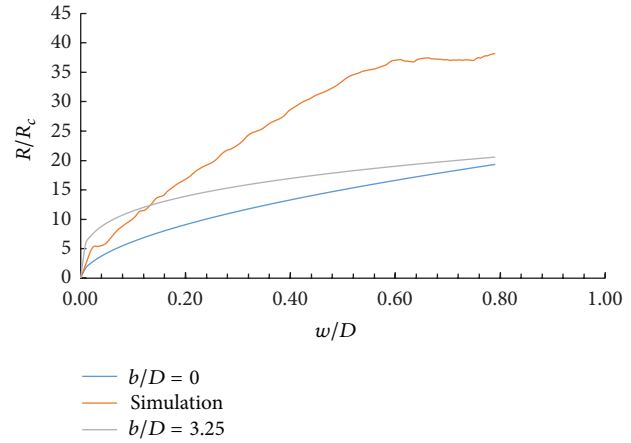

Figure 17: Comparison between Case A2 and NORSOK recommendations.

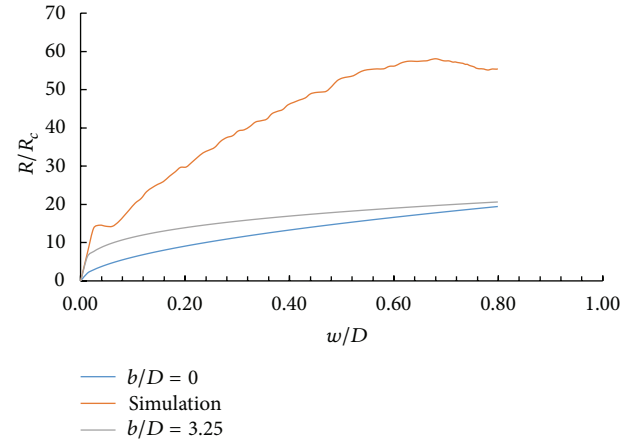

Figure 18: Comparison between Case A3 and NORSOK recommendations.

would undergo a large deformation, and a considerable amount of energy would be dissipated in the vessel itself. In the context of the present study of the platform's response to collisions, however, and to reduce the computation time, the rigid vessel model described in Part A was used.

3.2.1. Jacket Platform Model. Two platform models, model A and model B, were constructed. Model A was based on a platform in the South China Sea where the water depth was about 200 m (Figure 14). Model B was located in Bohai Bay, China, in water which was 70 m deep (Figure 15). Table 6 lists their principal dimensions. Platform A was flexible in global deformation mode; platform B was of more rigid construction.

Local indentation of the structural member in collision with the ship was of major concern in this study, along with the overall effect on the elastic deformation of the platforms; a fine finite element mesh was therefore generated for the model of the impacted leg segment. When complex loading was involved, the joint connections between structural members were more complex than the members themselves and were essential to the load-bearing capacity of the bracing members; thus, a fine mesh was generated for the joint connections also. For the two parts discussed above, four-node quadric element with global edge length 0.01 m was chosen. Only quad type mesh was used in the impacted leg segment to pursue a good calculation accuracy. Given the sophisticated shape of joint connections, however,

Table 5: Definition of collision cases.

Case	Vessel model	Leg segment model	Collision point
A1	Rigid	I	Mid-span
A2	Rigid	I	1/4-span
A3	Rigid	I	1/8-span
A4	Ductile	I	Mid-span
A5	Ductile	I	1/4-span
A6	Ductile	I	1/8-span
A7	Rigid	II	Mid-span
A8	Rigid	II	Lower end

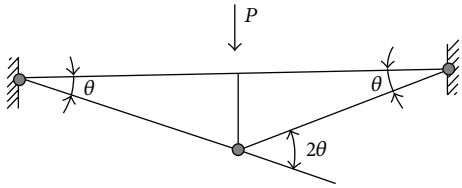

Figure 19: Three-hinge collapse mechanism for bracing element.

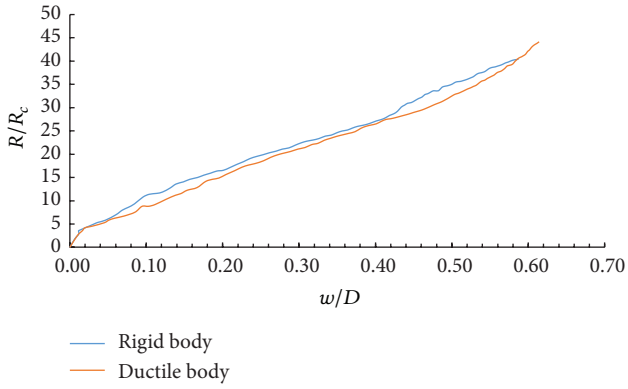

Figure 20: Comparison of resistance-indentation relationship between A1 and A4.

Table 6: Principal dimensions of jacket platforms.

Platform	A	B
Height	213 m	80 m
Section area (max)	18.5 m × 44.2 m	48 m × 48 m
Section area (min)	74 m × 74 m	48 m× 48 m
Topside weight	3600 t	2400 t
Water depth	200 m	70 m

Table 7: Platform model scenarios.

Case	Jacket model	Collision location on leg
B1	A	Mid-span
B2	A	1/4-span
B3	A	1/8-span
B4	A	Joint
B5	B	Mid-span
B6	B	Lower end

both quadric and triangle elements had to be used. A coarse mesh was used for other parts of the structure in order to minimize the computation time. This produced a total of 351784 elements for Platform A and 595305 elements for Platform B.

In practice, a considerable length of each jacket leg penetrated the foundation soil. This complicated the assessment of the lower boundary condition of the leg, since this must bear some relationship to the engineering properties of the soil; however, for the present purpose it was considered reasonable in both models to assume that the lower end of each leg was

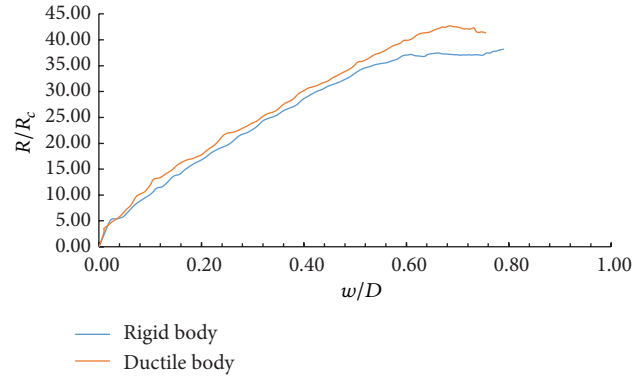

Figure 21: Comparison of resistance-indentation relationship between A2 and A5.

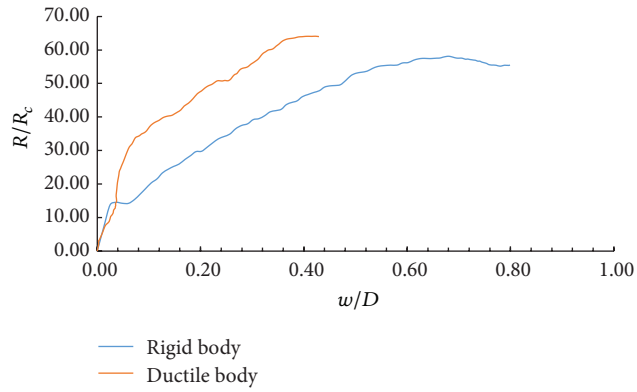

Figure 22: Comparison of resistance-indentation relationship between A3 and A6.

fixed. For both platform models, the boundary condition was applied at the areas where legs and soil connect.

The platform cases studied are defined in Table 7.

4. Results and Discussion

4.1. Assessment of NORSOK Standard N-004. The resistance-indentation relationship recommended by NORSOK Standard N-004 was compared with the numerical simulation results. For the sake of improving computation efficiency and reducing computation time, the rigid vessel model was adopted. The influence of vessel stiffness is discussed in Section 4.2. Since the tubular member was inclined, the contact area expanded as the colliding vessel continued to penetrate, making b/D continually increase. The resistance-indentation relationships for both maximum and minimum b/D values were considered. The resulting variation of the dimensionless resistance force with dimensionless indentation is shown in Figures 16, 17, and 18, in which w denotes indention, and R, R_c, and D are defined in NORSOK N-004.

The simulation results illustrated that the resistance initially rose sharply, then gradually decreased. For any given indentation, the corresponding resistance recommended by NORSOK N-004 was seen to be less than the value produced by the numerical simulation. In Figures 16–18, the deviation

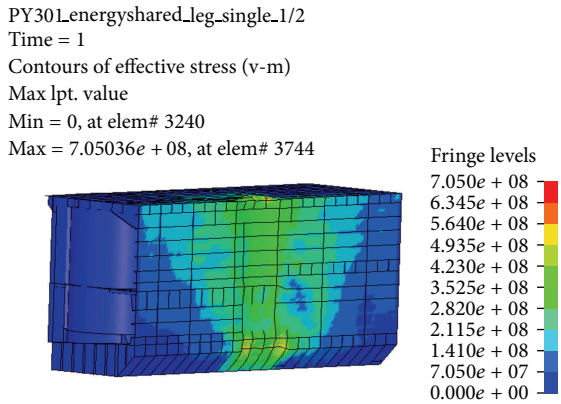

Figure 23: Vessel deformation, Case A4.

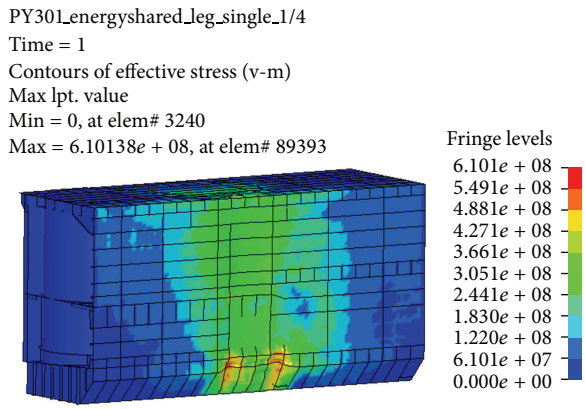

Figure 24: Vessel deformation, Case A5.

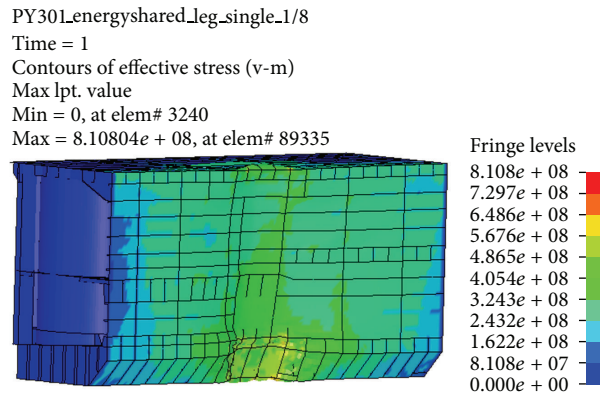

Figure 25: Vessel deformation, Case A6.

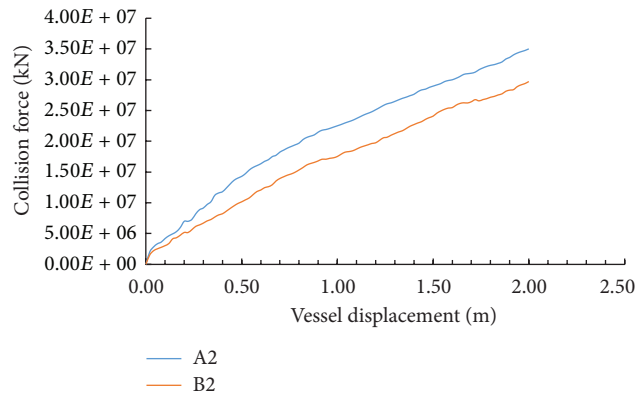

Figure 26: Collision force versus vessel displacement, mid-span collision.

from the NORSOK recommended value increased continuously with greater indentation.

According to Amdahl [1], the response of a tube subjected to lateral load consists of two stages. N-004 correctly describes the deformation behavior of the tube in initial stage, explaining the close agreement with the simulation results. As the tube underwent deflection, the load-bearing capacity increased rapidly due to a sharp rise in the membrane tensile force, accompanied by only a small increase in resistance. Obviously, N-004 is not able to represent the behavior of the tube at this stage. It is very difficult to analyze the interaction of local denting and deflection of a tubular member subjected to lateral impact load; however, it is both feasible and acceptable to treat the two deformation modes separately. Local denting around the impact point depends on the collision scenario—impact velocity, shape of colliding vessel, and so forth—making it impossible to resolve analytically. However, the rigid-plastic method of the analysis does provide acceptable analytical results of beam-type deformation. The simplest approach is the three-hinge collapse mechanism (Figure 19),

$$\frac{P}{P_0} = \sqrt{1 - \left(\frac{\omega}{D}\right)^2} + \frac{\omega}{D} \arcsin \frac{\omega}{D}; \quad \frac{\omega}{D} < 1,$$
$$\frac{P}{P_0} = \frac{\pi}{2}\frac{\omega}{D}; \quad \frac{\omega}{D} > 1, \tag{2}$$

where ω is the central deflection at the point of impact, D is the tube diameter, and P_0 is the failure load of the tube. It was assumed that the tube material develops fully plastic behavior. In addition, the strength of the joints must be adequate, especially if the impact point is close to a joint. The load-bearing capacity of the structure is drastically reduced if joints fail.

4.2. Influence of Shipside Stiffness on Resistance-Indentation Relationship. The simulated resistance-indentation relationships for different collision points were compared for the ductile- and rigid-vessel models (Figures 20–22). Note that indentation and resistance are both dimensionless quantities.

For the mid-span and 1/4 span collision cases, where only the unstrengthened section of the leg segment (wall thickness

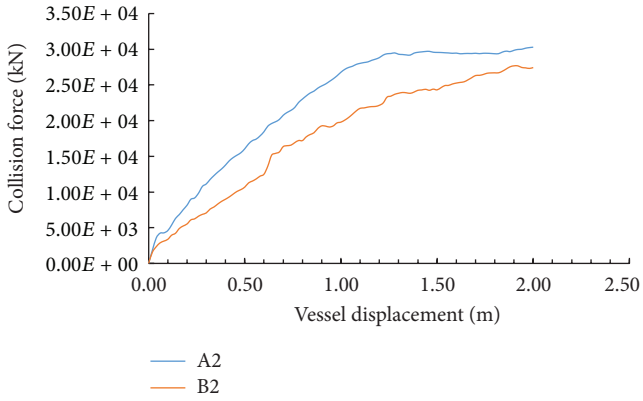

Figure 27: Collision force versus vessel displacement, 1/4 span collision.

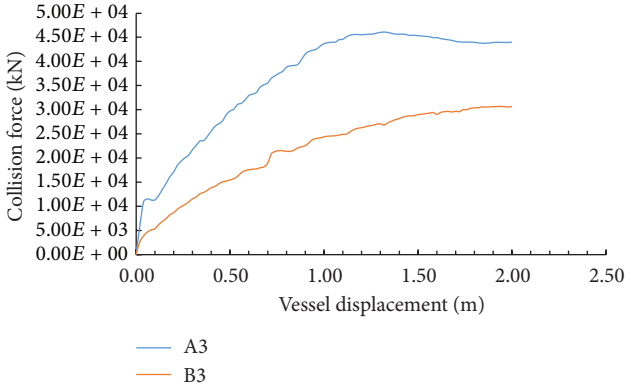

Figure 28: Collision force versus vessel displacement, 1/8 span collision.

Table 8: Maximum reductions in collision force.

Collision location	Mid span	1/4 span	1/8 span
Reduction	5370 kN	7110 kN	30700 kN

45 mm) underwent deformation, the resistance-indentation relationships of both vessel models were in close agreement (Figures 20 and 21). The ductile-vessel model showed little deformation, and little strain energy was dissipated within the vessel structure (Figures 23 and 24) and the plastic responses of the tubes were similar. However, a discrepancy appeared between cases A3 and A6: when the reference impact point was at 1/8 span, closer to the joint, and when the leg segment has been strengthened, the vessel was deformed appreciably (Figure 25). A relatively "soft" (i.e., low-strength ductile) vessel deforms more readily, therefore contributing to energy dissipation such that a much greater collision force would be required to produce a large impact energy affecting the leg segment. Thus, the gradient of the resistance-indentation relationship in Figure 22 tended to rise for the ductile-vessel model with relatively low hull strength.

4.3. Comparison of Collision Forces. It would be expected that the elastic response of the platform would alleviate the impact loads on members struck in a collision. Figures 26, 27, and 28 show comparisons of collision force versus vessel displacement between column A cases (Table 5) and platform A cases (Table 7).

For the same collision scenario, Figures 26–28 show that the collision forces for platform collision cases were less than those for single-leg segment collision cases, which demonstrates the buffering effect induced by the elastic response of the platform. The resistance of the affected structural member to large deformation is mainly attributable to membrane forces. Axial end conditions are especially important, since a lack of flexibility reduces the development of membrane forces. The global deformation of the platform offers some freedom of movement to the joints of the structural leg segments; as a result, the segment is flexibly fixed rather than rigidly fixed, and the collision forces occur due to inadequate development of membrane forces. The reduction in collision force depends on collision location. The maximum reductions are summarized in Table 8.

When the collision occurred close to joint connections, which were points of high local strength, there was a considerable reduction in the collision force, favoring the development of membrane tensile forces. The response of the

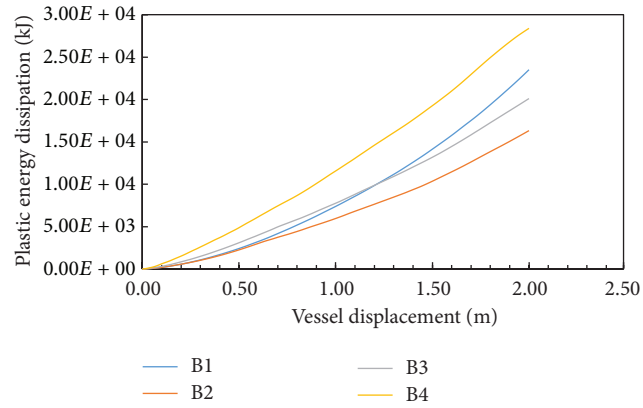

Figure 29: Plastic energy dissipation in structural member in collision, Platform A.

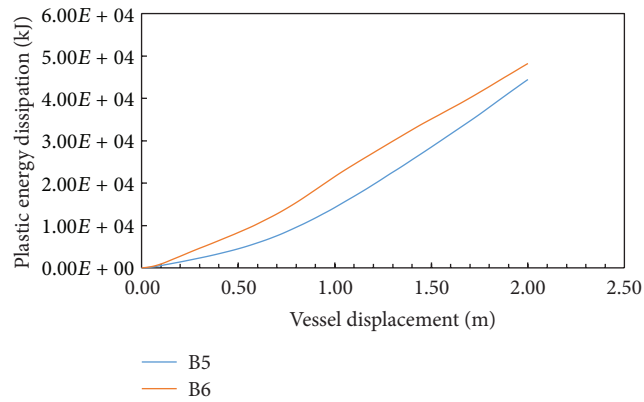

Figure 30: Plastic energy dissipation in structural member in collision, Platform B.

Table 9: Proportions of energy dissipation.

	Collision case	Elastic energy dissipation	Plastic energy dissipation
Platform A	B1	26.9%	73.1%
	B2	51.7%	48.3%
	B3	51.2%	48.8%
	B4	43.9%	56.1%
Platform B	B5	19.2%	80.8%
	B6	20.7%	70.3%

Table 10: Effect of topside mass on lag time.

Collision point	Platform A		Platform B	
	Topside mass (3600 t)	Topside mass (0 t)	Topside mass (2400 t)	
Mid-span	0.17 s	0.1 s	Mid-span	0.05 s
1/4 span	0.22 s	0.09 s		
1/8 span	0.11 s	0.06 s	Lower end	0.05 s
Lower joint	0.06 s	0.05 s		

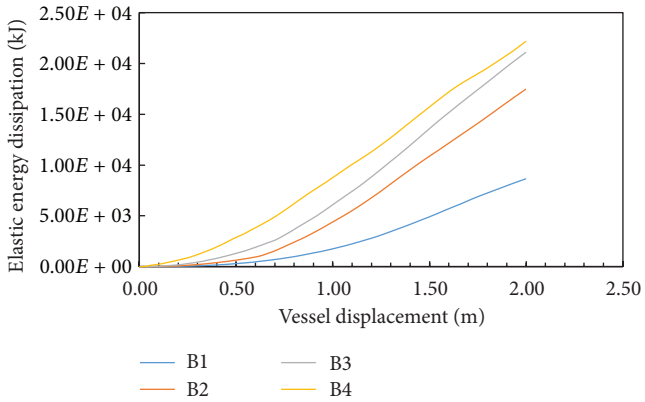

Figure 31: Energy dissipation in overall deformation, Platform A.

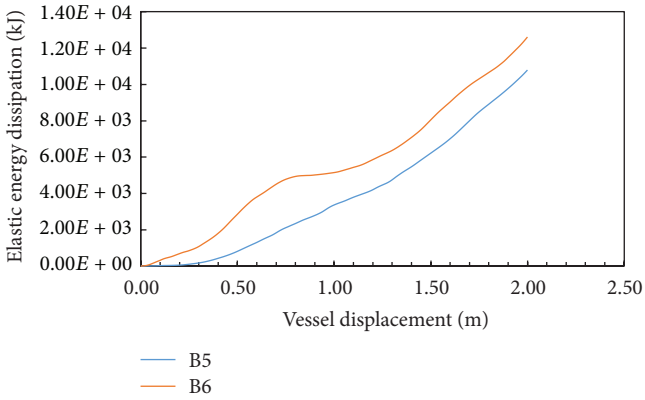

Figure 32: Energy dissipation in overall deformation, Platform B.

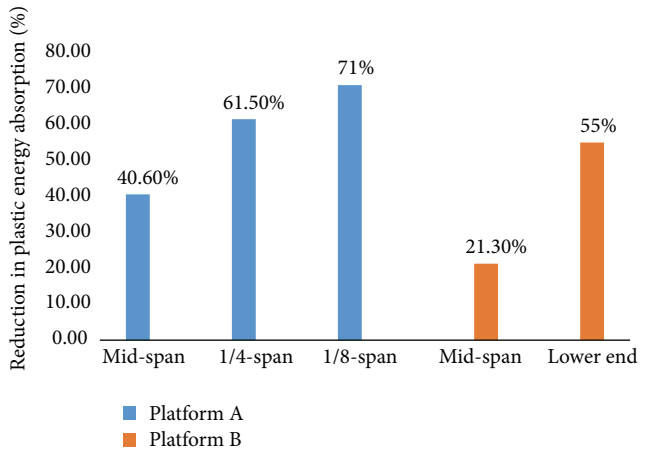

Figure 33: Reduction in local energy absorption.

platform to a collision then depends on its global deformation to a great extent, and a buffering effect is produced.

The buffering action did not occur immediately, however, but rather there was a lag time during which the reduction in impact load was negligible and the impacted member behaved as though it was rigidly fixed at both ends. This effect was mainly caused by the very large inertia of the platform topsides. The lag effect and the influence of topside weight on platform response are discussed in detail in Section 4.4.3 below.

4.4. Buffering Effect and Energy Dissipation. The impact energy is absorbed by the platform in various ways, depending on the relative stiffness and different deformation modes. The main emphasis here is on energy dissipation rather than collision force. The proportions of energy dissipation are summarized in Table 9. Elastic energy dissipation is considerable, especially for a flexible platform.

4.4.1. Plastic Energy Dissipation. The amount of energy absorbed locally by the affected member depends mainly on local cross-sectional deformation and beam-type deformation between its two ends. Figure 29 depicts the simulated

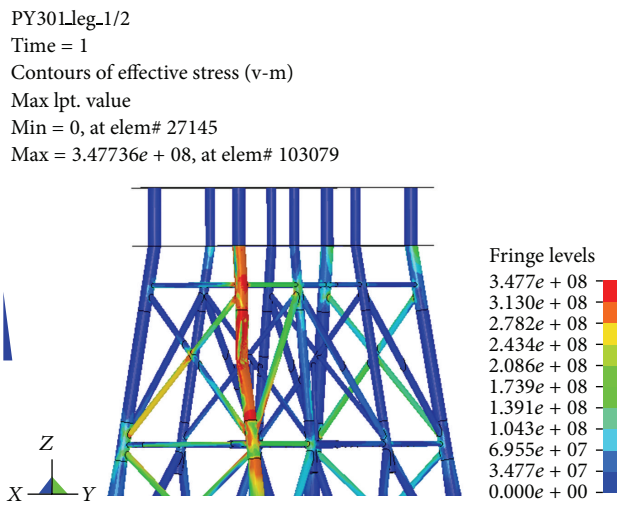

Figure 34: Local damage, Case B1.

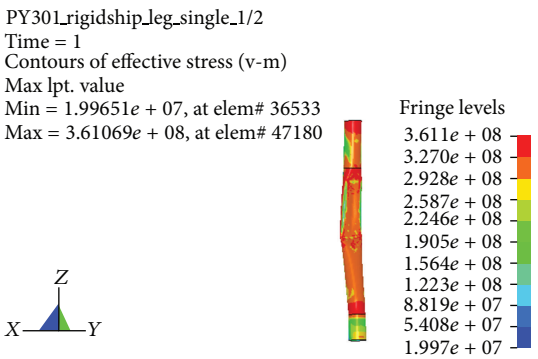

Figure 35: Local damage, Case A1.

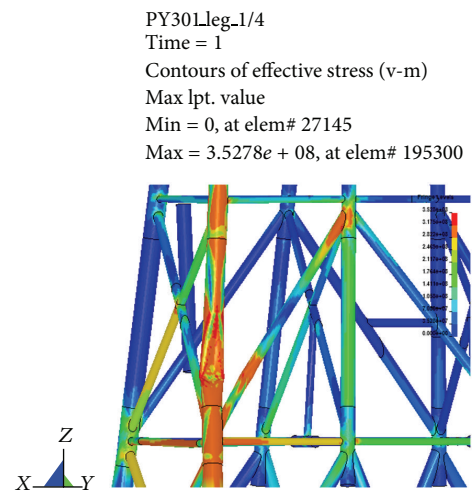

Figure 36: Local damage, Case B2.

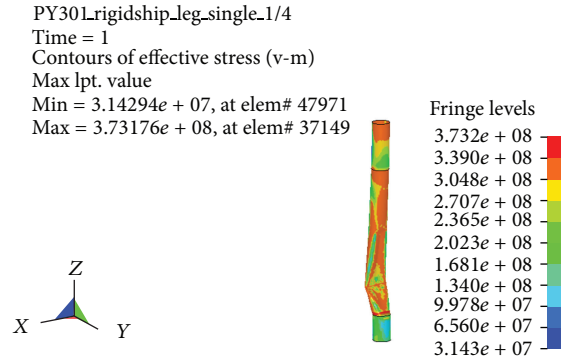

Figure 37: Local damage, Case A2.

local energy dissipation in the affected member for platform model A, with the proportion of energy dissipation in cross-sectional denting and beam-type deformation correlated with the point of collision. When the impact load (simulating the collision) was applied at the mid-span of the member, beam-type deformation was significant. Conversely, cross-sectional deformation was predominant when the load was applied close to a joint. Cross-sectional deformation was the main response in Cases B2, B3, and B4, in which energy dissipation depended mainly on the wall thickness in the vicinity of the impact point. Consequently, energy dissipation increased when the impact point was closest to thick-walled joints. However, in Case B1, the deformation behavior of the member was mainly beam-type bending and, even for small wall thicknesses, the energy dissipation was considerable.

Figure 30 depicts the simulated plastic energy dissipation in platform model B, which relied mainly on plastic response to bear the collision impacts. Such significant plastic response is believed to be caused by the relatively low local strength of structural members, considering that the design of Platform B is bulky in global deformation mode.

4.4.2. Elastic Energy Dissipation. Energy dissipation in members other than the leg segment impacted by the collision is shown in Figures 31 and 32, which indicate the elastic energy dissipated as a result of overall platform deformation. It can be seen that the amount of elastic energy dissipation remains low initially, then rises sharply along with ship displacement; this corresponds to the lag effect. Three-hinge mechanism analysis indicates that the membrane tensile forces developed most readily when the impact point was close to joints, where the impacted member is the strongest. The high local strength of members transmitting the forces to the topside favors an elastic response, as the topside rapidly dissipates kinetic energy. Comparison between Figures 31 and 32 shows a significant difference in the extent of elastic response of Platforms A and B. Regardless of the collision location, elastic energy dissipation in Platform B was found to be generally limited, which is mainly attributable to the very high overall stiffness of the structure.

The simulated buffering effect was reflected in the alleviation of collision forces and local energy dissipation, both of which contribute to the protection of the member impacted in the collision. Figure 33 summarizes the dimensionless reduction in plastic energy absorption, normalized for identical single-column cases.

It appears that obvious elastic response induces a large reduction in plastic energy absorption, reflecting a substantial buffering effect. When less plastic energy is dissipated,

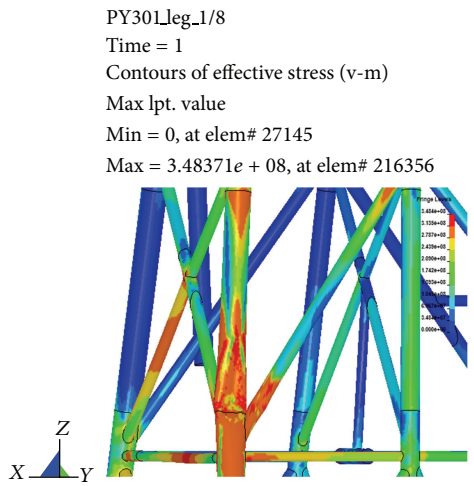

Figure 38: Local damage, Case B3.

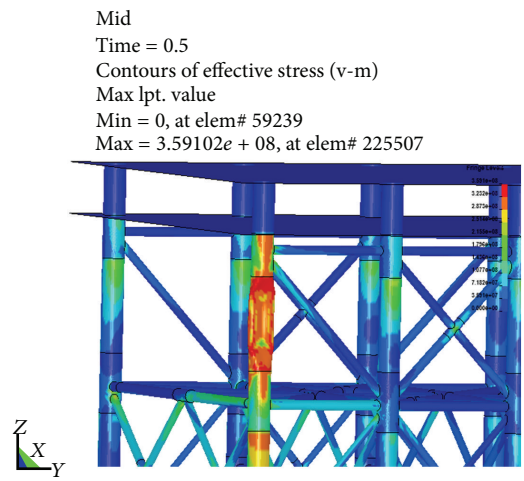

Figure 40: Local damage, Case B5.

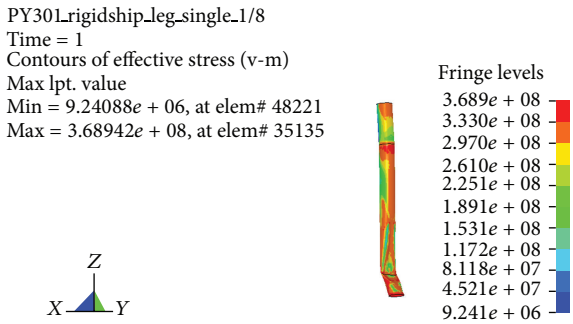

Figure 39: Local damage, Case A3.

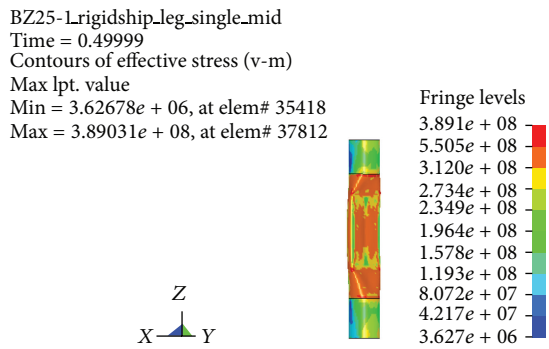

Figure 41: Local damage, Case A7.

impacted members are protected from undergoing severe structural damage. Figures 34 and 35 show the simulated local damage to the impacted member for Cases A1 and B1. For Case B1, maximum stress = 34.77 Mpa, maximum penetration = 0.8 m; for case A1, maximum stress = 36.11 Mpa, maximum penetration = 1.2 m. For the same collision scenario, the impacted member suffered less damage when the elastic response was considered. The other cases are illustrated in Figures 36, 37, 38, 39, 40, and 41.

The conclusions drawn from the above results are that, for structural members impacted by a collision, the impact force will decrease and less plastic energy is dissipated due to the elastic response of the platform, especially when the platform is flexible in global deformation mode. Furthermore, the members themselves suffer less structural damage.

In summary, the structural elements of a platform were shown in this study to be capable of withstanding a much more violent collision when the elastic response is considered, compared to an analysis where this aspect is ignored. All of these results demonstrate the buffering effect. It is logical, therefore, to point out that the NORSOK Standard N-004 underestimates the capacity of bracing elements to withstand collision impact.

4.4.3. Lag Effect. As foreshadowed in Section 4.3, the elastic response is time dependent, due to the very large inertia of the platform topside. The topside motion is directly coupled to overall deformation of the platform. The elastic response only becomes significant when sufficient impact energy has been transferred to the topside as kinetic energy. If the topside is constrained to zero degrees of freedom, the platform overall behaves as a beam rather than a cantilever.

The lag time denotes the period of time before the topside begins to deform. It is defined as the period of time when the topside velocity is less than 0.1 m/s. Due to its very large mass, the kinetic energy of the topside is also very large, even at low velocities. In order to investigate the effect of the topside mass on platform response, collision scenarios identical to Cases B1, B2, B3, and B4 above were defined, and the topside mass was manually set to zero. The lag times for the various cases are listed in Table 10. This demonstrates that the large topside mass increases the lag time considerably.

The length of the lag time correlates with factors such as collision location and platform size. Figures 42 and 43 depict the time histories of the topside kinetic energy of Platforms A and B for vessel collisions with different points on the structural member. It is shown that the lag time tends to be shorter when the impact point approaches joints in the structure. A high local strength of the impacted member transmitting the forces to the topside shortens the lag time. The elastic response for a bulky platform (e.g., platform B,

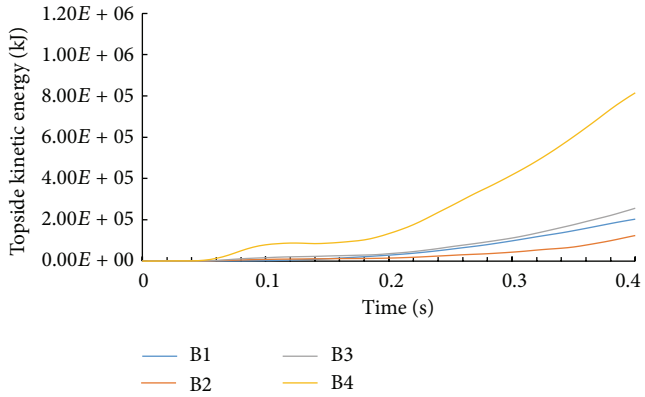

Figure 42: Time history of topside kinetic energy, Platform A.

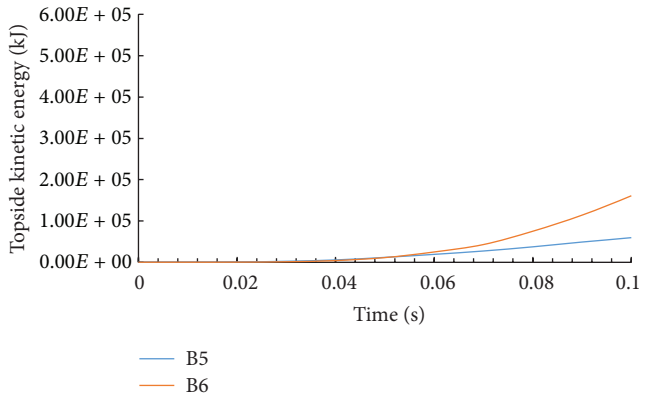

Figure 43: Time history of topside kinetic energy, Platform B.

Figure 43) is generally more rapid than for a flexible platform, regardless of the position of the collision point.

5. Conclusions

For large deformation, the resistance-indentation relationship recommended by NORSOK Standard N-004 underestimates the resistance to indentation caused in a shipside collision. This is due to an inaccurate description of the local deformation mode. Ship stiffness is important in the ship-column impact analysis, by influencing the distribution of energy dissipation. The gradient of the resistance-indentation relationship tends to increase when the ship's hull is relatively soft.

It is essential to be aware of the elastic response in the analysis of vessel-platform impacts. The contribution from the elastic response to alleviating collision forces and reducing energy absorption, defined in this paper as the buffering effect, is significant. In this way, bracing elements are protected from serious structural damage. Consequently, they are able to bear much more violent impacts than previously thought. A time delay exists during which buffering effect is negligible. This lag time effect occurs because the platform as a whole only deforms after the topside takes up sufficient kinetic energy to overcome its very large inertia.

The elastic response of a platform depends very much on where the colliding vessel strikes the leg segment of the platform. Collisions that occur close to joints favor the buffering effect, since the segment has greater local strength in that region. A platform that is flexible in global deformation mode tends to have a more marked buffering effect than a one that is nonflexible.

Acknowledgments

This work was supported by China Off-Shore Technology Center, ABS Great China Division, and Foundation of State Key Lab of Structure Analysis for Industrial Equipment, Dalian Technology University (Grant no. GZ1214), and Foundation of State Key Laboratory of Ocean Engineering, Shanghai Jiao Tong University (Grant no. GKZD010056-12); all of these supports are gratefully acknowledged by the authors.

References

[1] J. Amdahl, *Energy Absorption in Ship-Platform Impacts*, 1983.

[2] M. Zeinoddini, J. E. Harding, and G. A. R. Parke, "Effect of impact damage on the capacity of tubular steel members of offshore structures," *Marine Structures*, vol. 11, no. 4-5, pp. 141–157, 1998.

[3] M. Zeinoddini, J. E. Harding, and G. A. R. Parke, "Dynamic behaviour of axially pre-loaded tubular steel members of offshore structures subjected to impact damage," *Ocean Engineering*, vol. 26, no. 10, pp. 963–978, 1999.

[4] H. S. E. Visser Consultancy, *HSE-Science and Research-RR220-Ship Collision and Capacity of Brace Members of Fixed Steel Offshore Platforms*, Health and Safety Executive, 2004.

[5] J. Amdahl and E. Eberg, *Ship Collision With Offshore Structures*, Balkema, 1993.

[6] Y. Bai and P. Terndrup Pedersen, "Elastic-plastic behaviour of offshore steel structures under impact loads," *International Journal of Impact Engineering*, vol. 13, no. 1, pp. 99–115, 1993.

[7] P. T. Pedersen and S. Zhang, *On Impact Mechanics in Ship Collisions*, Danish Center for Applied Mathematics and Mechanics, Technical University of Denmark, 1998.

[8] O. Furnes and J. Amdahl, "Ship collisions with offshore platforms," in *Proceedings of the Intermaritec '80*, Hamburg, Germany, 1980.

[9] P. Gjerde, S. J. Parsons, and S. C. Igbenabor, "Assessment of jack-up boat impact analysis methodology," *Marine Structures*, vol. 12, no. 4-5, pp. 371–401, 1999.

[10] J. Waegter and M. J. Sterndorff, "Energy absorption in mono-tower platforms during ship collision," in *Proceedings of the 14th International Conference on Offshore Mechanics and Arctic Engineering*, pp. 235–243, June 1995.

[11] R. Watan, *Analysis and Design of Columns in Offshore Structures Subjected to Supply Vessel Collisions*, Norwegian University of Science and Technology, 2011.

[12] L. Hong, *Simplified Analysis and Design of Ships Subjected To Collision and Grounding*, Norwegian University of Science and Technology, 2009.

[13] S. Zhang, *The Mechanics of Ship Collisions*, Institute of Naval Architecture and Offshore Engineering, 1999.

[14] G. Wang, *Structural Analysis of Ship Collision and Grounding [Ph.D. thesis]*, University of Tokyo, 1995.

[15] API R P. 2A-WSD, Recommended Practice for Planning, Designing, and Constructing Fixed Offshore Platforms-Working Stress Design, 2000.

[16] Standards Norway. NORSOK STANDARD N-004.